NIH Public Access
Author Manuscript
FEBS J. Author manuscript; available in PMC 2010 August 1.

Published in final edited form as:
FEBS J. 2009 August ; 276(16): 4505–4514.

Fast Ferrous Heme-NO Oxidation in Nitric Oxide Synthases

Jesús Tejero, **Jérôme Santolini**[1], and **Dennis J. Stuehr**
From the Department of Pathobiology, Lerner Research Institute, Cleveland Clinic Foundation, Cleveland, Ohio 44195.

Abstract

During catalysis, the heme in nitric oxide synthase (NOS) binds NO before releasing it to the environment. Oxidation of the NOS ferrous heme-NO complex by O_2 is key for catalytic cycling, but the mechanism is unclear. We utilized stopped-flow methods to study reaction of O_2 with ferrous heme-NO complexes of the inducible and neuronal NOS enzymes. We found that the reaction does not involve heme-NO dissociation, but instead proceeds by a rapid, direct reaction of O_2 with the ferrous heme-NO complex. This behavior is novel and may distinguish heme-thiolate enzymes like NOS from related heme proteins.

Keywords

Heme protein; heme-thiolate; nitric oxide; redox; enzyme mechanism

Introduction

Nitric oxide (NO) is a signaling and effector molecule in the neural, vascular, and immune systems [1]. Three related NO synthases (NOS, EC 1.14.13.39) generate NO from L-arginine in mammals; inducible NOS (iNOS), endothelial NOS (eNOS), and neuronal NOS (nNOS) [2–5]. NOS-like enzymes also exist in some gram-positive bacteria [6;7]. All NOS are homodimers, and each subunit consists of an N-terminal oxygenase domain that binds iron protoporphyrin IX (heme), 6*R*-tetrahydrobiopterin (H_4B), and L-arginine (L-Arg) and a C-terminal reductase domain that binds FMN, FAD, and NADPH. The two domains are connected to one another by an intervening calmodulin binding sequence [2].

An interesting feature of NOS catalysis is that the newly-synthesized NO binds to the heme prior to release from the enzyme [8;9]. Therefore, the end product of the reaction is not NO but heme Fe^{III}-NO. During catalysis, this product complex can become reduced by the NOS reductase domain to heme Fe^{II}-NO at a rate comparable to that of Fe^{III}-NO dissociation. This leads to two possible fates for each new NO molecule: release from the heme Fe^{III}-NO complex into solution (productive cycle) or oxidation through the reaction of the heme Fe^{II}-NO complex with O_2 (futile cycle). We have proposed a global mechanism for NOS catalysis that takes these facets into account (Fig. 1) [10;11]. Kinetic measurements of the individual steps revealed that the catalytic behavior of any NOS is primarily characterized by the interplay of three kinetic parameters; namely *kr* (the rate of Fe^{III} (or Fe^{III}-NO)-heme reduction by the reductase domain), *kd* (the dissociation rate of NO from the heme Fe^{III}-NO complex) and *kox* (the oxidation rate of the heme Fe^{II}-NO complex) [3;10;11] (Fig. 1).

Corresponding author: Dennis J. Stuehr, Department of Pathobiology (NC-22), The Cleveland Clinic, Foundation, Lerner Research Institute, 9500 Euclid Ave., Cleveland, OH 44195. Tel.: 216-445-6950; Fax: 216-636-0104; stuehrd@ccf.org.
[1]Present address: Laboratoire de Stress Oxydant et Détoxication, iBiTec-S, Commissariat à l'Energie Atomique, Saclay, Gif-sur-Yvette 91191 Cedex, France

NIH-PA Author Manuscript
NIH-PA Author Manuscript
NIH-PA Author Manuscript

NIH-PA Author Manuscript NIH-PA Author Manuscript NIH-PA Author Manuscript

Computer simulations of the global mechanism, and characterization of various eNOS and nNOS mutants that have altered kinetic parameters, has shown that the NO synthesis activity and apparent $K_M O_2$ of a NOS enzyme can be significantly dependent on the *kox* rates [12].

Despite the importance of *kox*, the reaction of the NOS heme Fe^{II}-NO complex with O_2 has not been the object of specific studies, and *kox* rates have only been determined for NOS enzymes at 140 μM oxygen (half air-saturated conditions). Here, we utilized stopped-flow spectroscopy to study the oxidation reaction of the iNOS and nNOS heme Fe^{II}-NO complexes at different O_2 concentrations. Our results show: (i) NOS heme Fe^{II}-NO complexes oxidize at much higher rates than those reported for any other heme protein, (ii) the NOS oxidation mechanism does not involve NO dissociation from the heme, and instead involves a direct reaction of O_2 with heme-bound NO. These novel facets of heme-NO reactivity fundamentally distinguish heme-thiolate enzymes like NOS from hemoglobins and related enzymes.

Results

Heme Fe^{II}-NO Dissociation rates

We studied NO dissociation from pre-formed ferrous heme-NO complexes of iNOSoxy and nNOSoxy, using sodium dithionite as an NO scavenger in the presence of CO. When NO dissociates from the NOS heme, CO binds quickly [20–23] to form a heme Fe^{II}-CO complex, which can be followed by a shift in the heme Soret absorbance from 436 nm to 445 nm. Spectral analysis of the NO dissociation reactions for nNOSoxy and iNOSoxy are shown in Figure 2. In both cases the absorbance increase at 445 nm (Figures 2C–D) fit well to a single exponential equation and the transitions show isosbestic points consistent with a single step process (Figures 2A–B). The NO dissociation constants obtained were $3.9 \pm 0.6 \times 10^{-4}$ s^{-1} (nNOSoxy) and $1.0 \pm 0.1 \times 10^{-4}$ s^{-1} (iNOSoxy), similar to previously reported values of 3.1×10^{-4} s^{-1} and 1.35×10^{-4} s^{-1} for nNOS [16] and iNOS [11], respectively. Because the NO dissociation rates are 3 to 4 orders of magnitude slower than the *kox* values reported for iNOSoxy and nNOSoxy at half-air saturation, (*kox* of 3.0 s^{-1} and 0.19 s^{-1} for iNOS and nNOS, respectively) [11;12] we conclude that an NO dissociation step is not involved in the oxidation mechanism of NOS heme Fe^{II}-NO complexes.

Oxygen dependence of kox and possible buildup of reaction intermediates

We utilized stopped-flow spectroscopy to study the oxidation reactions of pre-formed iNOSoxy and nNOSoxy heme Fe^{II}-NO complexes at different oxygen concentrations, to determine the oxygen dependence of *kox* and to observe if any heme-based reaction intermediates would build up. Figure 3A contains representative spectral data collected during reaction of the iNOSoxy Fe^{II}-NO complex with 170 μM oxygen in the presence of both H_4B and L-Arg. The spectral changes are consistent with conversion of the Fe^{II}-NO complex into the Fe^{III} high-spin form of iNOSoxy. The reaction here was well-described as a single step process, as indicated by the several isosbestic points in the spectra (Fig. 3A) and by the single exponential decay of the absorbance signal at different wavelengths (Fig. 3A, inset). The rate of Fe^{II}-NO complex disappearance (437 nm) was similar to the rate of ferric enzyme product formation (396 nm) (Fig. 3A, inset). The spectral and fitting results we obtained for replica reactions run at other O_2 concentrations were highly similar. In all cases, the reactions proceeded as single step processes with no apparent buildup of enzyme reaction intermediates. The plot of the observed rates (*kox* values) versus oxygen concentration shows a linear dependency across the entire range of experimental O_2 concentrations (Figure 4A), and did not display saturation kinetic behavior. From the plot, rate constants for the bimolecular reaction (k_1 and k_{-1}, see methods) were obtained. There was no substantial change in the accuracy of fit when the k_{-1} term was not included, and

NIH-PA Author Manuscript

therefore we assume that it is too small to be accurately determined by our method. A k_1 value of 26500 ± 340 $M^{-1}s^{-1}$ was calculated for the reaction of the iNOSoxy heme Fe^{II}-NO complex with O_2 (Table 1). We used the same procedure to analyze the reaction of the nNOSoxy heme Fe^{II}-NO complex with O_2. Fig. 3B contains representative spectra recorded for reaction of the complex with 170 μM O_2 in the presence of both L-Arg and H_4B. The overlapped spectral traces create isosbestic points at approximately the same wavelengths as we observed in the iNOSoxy reactions. The reactions of nNOSoxy were also single exponential and showed no detectable buildup of enzyme intermediates in any case. When the observed rates were plotted versus O_2 concentration a linear dependency was observed (Fig. 4B) with no saturation across the entire experimental O_2 concentration range. The calculated rate constants were k_1 = 230 ± 8 $M^{-1}s^{-1}$ and k_{-1} = 0.047 ± 0.004 s^{-1} (Table 1). Thus, reaction of the nNOSoxy heme Fe^{II}-NO complex with O_2 exhibited similar behavior to that of the iNOSoxy heme Fe^{II}-NO complex, but was about 100 times slower at any given O_2 concentration (compare Fig. 3B (inset) and Fig. 4B).

Nitrate and nitrite product formation

To quantify product formation, the iNOSoxy Fe^{II}-NO complex was formed and purified under anaerobic conditions (see Methods). Aliquots were mixed with air saturated buffer and the amounts of NO_2^- and total $NO_2^- + NO_3^-$ were quantified by chemiluminescence and photometric assays (see methods). Percent values were calculated dividing the concentration of the nitrite/nitrate species by the initial concentration of NOS in each sample and multiplying by 100 the resulting value. Thus, a 100% value is equivalent to 1 mole of nitrite/nitrate produced per mole of enzyme. The results are shown in Figure 5. The detected amounts of nitrite or total nitrite plus nitrate were: NO_2^- = 17.0 ± 1.4 %; Total NO_2^-/NO_3^- = 123 ± 10 % (iNOS) and NO_2^- 15.7 ± 0.6 %; Total NO_2^-/NO_3^- = 116 ± 15% (nNOS). Thus, the results with both enzymes were similar with approximately 1 mole of nitrate and 0.2 moles of nitrite produced per mole of Fe^{II}-NO complex. Some possible sources of the small amount of NO_2^- can be the reaction of excess NO with O_2 or reduction of NO_3^- by excess dithionite. On the other hand, NO_3^- can only be formed in the enzymatic reaction via the futile cycle (see Fig. 1). We conclude that the reaction of the NOS ferrous-NO complexes with oxygen leads quantitatively to nitrate.

Discussion

The reaction of O_2 with the ferrous heme-NO complexes of hemoglobin and myoglobin have been closely studied and serve as a paradigm for our present study [24–26]. A central hallmark of these reactions is that they are relatively slow and proceed at rates that basically match their rates of heme Fe^{II}-NO dissociation (Table 1, [26]). This has led to a generally accepted mechanism illustrated in Fig. 6 (top portion), where NO dissociation from the ferrous heme is the initial and rate-limiting step for the overall oxidation. In these cases, NO dissociation allows O_2 to bind to the ferrous heme and form a heme Fe^{II}-O_2 complex, which then reacts rapidly with NO. This reaction appears to take place inside the heme pocket [26;27], as indicated by the rate being pH-independent and mono-molecular, and no nitrite being formed as product, which could otherwise result if any NO was released from the protein into solution.

For NOS enzymes, the mechanism of heme Fe^{II}-NO oxidation by O_2 does not involve an NO dissociation step, because the observed rates of heme Fe^{II}NO dissociation are two or three orders of magnitude slower than the observed rates of heme Fe^{II}NO oxidation. Our results suggest two alternative reaction mechanisms that are illustrated in Fig. 6. Both have O_2 reacting directly with the NOS heme Fe^{II}-NO complex, in one case as an electrophile that attacks the nitrogen of the bound NO (k_1/k_{-1}) and in the other case as an oxidant in an outer-sphere electron transfer reaction (k_1'/k_{-1}') that generates heme Fe^{III}-NO and

NIH-PA Author Manuscript NIH-PA Author Manuscript NIH-PA Author Manuscript

superoxide. In either case, the initial O_2-dependent reaction appears to be the rate-limiting step, and conceivably both reactions would generate an *N-bound* heme-peroxynitrite complex as an immediate product (Fig. 6). Because we observed monophasic transitions for our iNOSoxy and nNOSoxy reactions with no apparent build-up of a heme-peroxynitrite product complex, this suggests that the immediate heme-product complex may dissociate (or rearrange) relatively quickly to form the observed ferric enzyme product (Fig. 6). This is consistent with the reaction rates not saturating even at the highest O_2 concentrations that were experimentally available to us. Interestingly, buildup of an observable oxo-ferryl heme intermediate does occur when excess peroxynitrite is reacted with ferric iNOSoxy [28]. However, this reaction involves the initial formation of an *O-linked* heme-peroxynitrite complex, which is not likely to form in our reactions.

The outer-sphere electron transfer mechanism depicted in Fig. 6 (k_1'/k_{-1}') is likely to be thermodynamically uphill based on a comparison of the midpoint potentials for the $O_2/O_2^{\,-}$ couple (−330 mV) [29] versus the NOS Fe^{III}-NO/Fe^{II}-NO couple (−2 mV) [30]. However, the equilibrium could be driven toward products if the subsequent reaction of superoxide and the heme Fe^{III}-NO complex is fast. This pathway would form the same *N-bound* heme-peroxynitrite intermediate as in the mechanism proposed above. If an outer-sphere electron transfer occurs, it opens up the possibility that NO could dissociate from the heme Fe^{III}-NO complex prior to reaction with superoxide (Fig. 6). However, the measured rates of NOS heme Fe^{III}-NO dissociation (*kd*) range from 2 to 60 s^{-1} at similar temperatures [8;11;31]. Therefore, the probability of NO escape from the enzyme would depend on the initial O_2 reaction proceeding by an outer-sphere electron transfer, and the resulting superoxide exhibiting a poor reactivity toward the heme Fe^{III}-NO complex. We believe this combination of events is unlikely. Instead, the heme Fe^{II}-NO complex of iNOSoxy and nNOSoxy appears to undergo an efficient NO dioxygenase reaction to generate nitrate with little or no NO escaping from the enzyme during the reaction.

What makes the heme Fe^{II}-NO complexes of iNOSoxy and nNOSoxy more reactive toward O_2 than the heme Fe^{II}-NO complexes of Hb or Mb? A difference in O_2 access is not likely to be involved, because each of these heme proteins evolved to bind O_2, and their ferrous forms all have fairly similar *kon* values for O_2 and for other diatomic ligands [13;30;32]. Instead, the difference may be caused in part by the heme-thiolate bond causing the NOS heme Fe^{II}NO complex to have a lower midpoint potential. The midpoint potential of the Fe^{III}NO/Fe^{II}NO couple in NOS (−2 mV) [30] is about 50 to 150 mV more negative than the same couple in histidine-ligated heme proteins [33]. Resonance Raman data are consistent with greater electron density in the NOS heme-NO complexes compared to globins, and suggest the bound NO exhibits some nitroxide-like character, which should increase its reactivity toward O_2 if the mechanisms proposed in Fig. 6 are accurate. Conceivably, one might further increase the oxidation rate of a heme Fe^{II}-NO complex by O_2 by further decreasing the heme midpoint potential. This effect may have been achieved for the W409F mutant of nNOS, whose more negative Fe^{III}/Fe^{II} midpoint potential is associated with a 7-times faster *kox* than in wild-type nNOS [12]. In general, different heme proximal ligands (cysteine *versus* histidine) or related protein modifications near the heme may enable a range of heme midpoint potentials. At one extreme (more positive potential), this may diminish the O_2 reactivity of a protein's heme Fe^{II}-NO complex to such an extent that consecutive NO dissociation and O_2 substitution steps dominate the oxidation mechanism (as for Hb and Mb). At the other extreme (more negative potential), it may increase the O_2 reactivity of a protein's heme Fe^{II}-NO complex enough to enable a direct and potentially faster oxidation reaction (as in NOS enzymes). Layered onto this "redox" regulation are likely to be effects from other aspects of protein structure that together will determine the mechanism and kinetics of heme Fe^{II}-NO oxidation for any given protein.

NIH-PA Author Manuscript NIH-PA Author Manuscript NIH-PA Author Manuscript

Recent evidence suggests that histidine-ligated heme proteins may exhibit a range of behaviors regarding the O_2 oxidation of their heme Fe^{II}-NO complexes [34]. For example, the hexacoordinate heme proteins neuroglobin and hemopexin show interesting differences with the aforementioned Hb and Mb. The reactions of hemopexin or neuroglobin heme Fe^{II}-NO complexes with O_2 proceed relatively fast and they form what appear to be detectable heme-peroxynitrite intermediates that have relatively slow conversion rates to ferric enzyme [34–36]. The reported rates are compared in Table 1. Interestingly, the heme Fe^{III}/Fe^{II} midpoint potentials of hemopexin and neuroglobin are more negative than those of Hb and Mb, consistent with the concept of redox regulation as described above. Flavohemoglobins are another type of histidine-ligated heme protein that catalyze an NO dioxygenase reaction to form nitrate [37;38]. Their reaction is extremely fast with a k_{cat} of 112–670 s^{-1} at 37°C [39;40]. The bulk of evidence suggests the their mechanism involves ligand substitution on the ferrous heme (O_2 for NO) as described for reactions of the heme Fe^{II}-NO complexes of Mb and Hb in Fig. 6 [37;41–43]. This would imply an unusually fast NO dissociation from the flavohemoglobin heme Fe^{II}-NO complex. Recently, fast NO dissociation rates were observed (43.5 s^{-1} at 20 °C) [44] for the heme Fe^{II}-NO complex of cytochrome cd_1, which appears to explain its fast steady-state activity [44;45]. Apparently, broad variations in NO *kd* and/or in heme midpoint potential may help to determine the mechanism and speed by which various heme protein Fe^{II}-NO complexes are oxidized by O_2. These concepts merit further investigation.

Concluding remarks

NOS enzymes catalyze a more rapid oxidation of their heme Fe^{II}-NO complex than any other heme-containing protein that has been studied to date. The basis is likely related to their heme environment, and particularly to the characteristics of the heme-thiolate bond. Further studies are under way to test the importance of heme midpoint potenial, heme distortion, NOS quaternary structure (dimer versus monomer), heme pocket access, active site residues, and the influence of bound cofactor or substrate. Because NOS form a heme Fe^{II}-NO complex during their normal catalytic cycle it may have forced them to develop a way to efficiently oxidize these complexes, which otherwise can constitute a dead-end in catalysis. Other heme-thiolate proteins appear to show differences in their NO reactivity [46], and many cytochrome P450's are inactivated by NO [47;48]. It will be interesting to see if the reaction described here for NOS is applicable to other heme-thiolate proteins.

There is a remarkable difference between iNOSoxy and nNOSoxy in their rates of their heme Fe^{II}-NO oxidation. The fast oxidation of the iNOS heme Fe^{II}-NO complex could be designed to synthesize peroxynitrite. This would be in accord with a physiological role of iNOS in host defense, and might help to explain why protein nitration is observed in some cells upon iNOS expression [28;49;50]. In this context, it is interesting to note that the bacterial NOS-like enzymes from *Deinococcus radiodurans* [51] and *Streptomyces turgidiscabies* [52] have both been found to catalyze amino-acid nitration. In comparison, the relatively slower oxidation of the nNOS heme Fe^{II}-NO complex has been suggested to enable its function in biological O_2 sensing [53;54] or to serve as a pulse source of NO in signal transduction cascades [55]. Our current work provides a foundation to test these possibilities.

Materials and methods

Reagents

O_2 and N_2 (medipure grade) gases were obtained from Praxair. NO gas was purchased from Linde LLC. H_4B was purchased from Schircks Laboratories (Jona, Switzerland). Glacial

NIH-PA Author Manuscript NIH-PA Author Manuscript NIH-PA Author Manuscript

acetic acid was purchased from Mallinckrodt Baker. Other chemicals were obtained from either Fisher Scientific (Pittsburgh, PA) or Sigma (St. Louis, MO).

Protein purification

The oxygenase domains of rat nNOS and mouse iNOS were overexpressed in *E. coli* and purified as previously described [13;14]. Protein concentration was determined from the absorbance at 444 nm of the ferrous-CO complex using an extinction coefficient of 74 $mM^{-1}cm^{-1}$ [15].

Ferrous heme-NO dissociation rates

The dissociation rates of NO from ferrous heme-NO complexes were studied in the presence of CO and using sodium dithionite as an NO scavenger as described [11;16]. The rate for the reaction of dithionite with NO is 1.4×10^3 $M^{-1}s^{-1}$ at 20 °C in 50 mM phosphate buffer at pH 7.0 [17]. Although oxyhemoglobin is a more efficient NO scavenger, dithionite has been successfully used when NO dissociation is a slow process, such as for ferrous-NO complexes of hemoglobin or NOS [11;16;17]. Solutions of iNOSoxy or nNOSoxy (40–80 μM) were made anaerobic in the presence of 2.5 mM L-Arg, 20 μM H_4B, 1 mM DTT in EPPS 40 mM pH 7.6 buffer were made anaerobic and then the ferrous heme-NO complexes were formed by adding successively sodium dithionite (final concentration 1.5 mM) and NO from a saturated NO-solution in EPPS buffer (final concentration 200 μM, NO saturated buffer concentration is 2.05 mM at 20 °C). The reaction was studied at 10 °C and was started by adding 100 μl of ferrous heme-NO solution to 900 μl of CO-saturated EPPS 40 mM, pH 7.6 buffer containing 2.5 mM L-Arg, 20 μM H_4B, 1 mM DTT and 1.5 mM dithionite. The conversion of the heme Fe^{II}-NO complex to the Fe^{II}-CO complex was monitored by UV-Visible spectroscopy and changes at 445 nm were fit to single exponential equations using Origin Pro 7.5 software (OriginLab, Northampton, MA).

Ferrous heme-NO oxidation

Ferrous heme-NO complexes were prepared as follows: protein solutions containing 10 μM of ferric NOS were prepared in 40 mM EPPS buffer, pH 7.6, 10% Glycerol, 150 mM NaCl, 0.5 mM EDTA, 20 μM H_4B and 2.5 mM L-Arg. Samples were made anaerobic in sealed cuvettes by several cycles of nitrogen/vacuum. Then, Fe^{III}-heme was titrated with sodium dithionite to produce the ferrous enzyme. Reduction of the enzyme was monitored in either a Cary 100 or a Shimadzu UV-2401 PC spectrophotometer. Ferrous enzyme was then titrated with a NO-saturated buffer solution. Each Fe^{II}-NO complex was then transferred to a syringe housed in a temperature-controlled Hi-Tech SF-61 stopped-flow instrument (Hi-Tech Scientific, Salisbury, UK) equipped with a diode array detector. The NOSoxy Fe^{II}-NO complex was rapidly mixed with O_2-containing buffer with the same composition as the protein buffer. Reactions were carried out at 10 °C. To assess the oxygen-dependency of the reaction, variable concentrations of oxygen were produced by mixing different amounts of O_2-saturated and N_2-saturated buffers. The concentration of oxygen in the O_2 saturated buffer at 10°C was calculated to be 1.7 mM [18]. As the mixing ratio was 1:1 the final O_2 concentration achieved varied from 0 to 850 μM.

Kinetic analysis

Reaction rates were calculated from the absorbance changes at the wavelength of the Soret peaks of Fe^{III}-heme (≈ 396nm, ferric heme recovery) or heme Fe^{II}-NO (≈ 436nm, ferrous heme-NO decay). Data were fitted to a single-exponential equation. The oxygen dependency of the observed rates versus O_2 concentration was fit to a linear equation in the form: $k_{obs} = k_1 [O_2] + k_{-1}$, were k_1 and k_{-1} are the apparent rates of O_2 association and dissociation, respectively. For iNOSoxy the value of k_{-1} is too small to be determined accurately and a

linear fit through zero in the form $k_{obs} = k_1 [O_2]$ was used. Data analysis was carried out using Origin Pro 7.5 software (OriginLab, Northampton, MA).

Determination of end products

iNOSoxy and nNOSoxy samples (approx 80 μM) were prepared in 40 mM EPPS buffer, pH 7.6, 10% Glycerol, 150 mM NaCl, 0.5 mM EDTA, 200 μM H_4B and 2.5 mM L-Arg. The ferrous-NO complex was formed by successive titrations with sodium dithionite (to form ferrous enzyme) and NO-saturated buffer as described above. In order to minimize generation or carryover of oxidized nitrogen species from the excess dithionite and NO, the cuvettes were next transferred to a glove-box (Belle Technology, Portesham, Dorset, UK) that was kept below 10 ppm O_2 and the ferrous-NO proteins were run through a Sephadex G-25 column (PD-10, GE Healthcare) equilibrated in anaerobic EPPS buffer 40 mM, pH 7.6, 10% Glycerol, 150 mM NaCl. The eluted fractions were transferred again to an anaerobic cuvette to determine their final concentrations (20–30 μM) and to insure that NO had remained bound to ferrous heme. Then the ferrous-NO complexes were mixed with different amounts of air-saturated buffer (final protein concentrations 5–25 μM). Nitrite and total nitrite plus nitrate (NOx) concentrations in the samples were measured using chemiluminescence as previously described [19]. Before measurement, samples were pretreated with 10% w/v ZnSO4 and 0.5 N NaOH and centrifuged to remove protein. Nitrite was converted to NO in line during the measurement by a solution containing an excess of potassium iodide in glacial acetic acid. Total NOx was converted to NO by a saturated solution of VCl_3 in 1 M HCl. NO generated was detected by the Sievers NOA 280i (GE Analytical Instruments, Boulder, CO). All samples were measured at least in triplicate and the nitrite and NOx concentrations were determined by interpolation using authentic standards of nitrite and nitrate, respectively. Additional measurements of nitrite and total nitrite and nitrate (NOx) concentrations were carried out photometrically using the Griess assay on the same samples. The protein was removed from the samples by centrifugation through Amicon Ultra centrifugal devices with a 10 kDa MW cut-off (Millipore). In this case, to estimate the total amount of nitrite plus nitrate the samples were reduced by a cadmium-copper catalyst (Nitralyzer II, World Precision Instruments, Sarasota, FL, USA) and assayed following the procedure provided by the supplier.

Abbreviations

EDTA ethylene diamine tetraacetic acid

EPPS 4-(2-hydroxyethyl)-1-piperazinepropanesulfonic acid

Fe^{II}-NO ferrous heme-NO complex

Fe^{III}-NO ferric heme-NO complex

FAD flavin dinucleotide

FMN flavin mononucleotide

H_4B (6R)-5,6,7,8-tetrahydro-L-biopterin

kr reduction rate of the heme by the reductase (flavoprotein) domain of NOS

kd dissociation rate of NO from the ferric heme-NO complex of NOS

kox oxidation rate of the ferrous heme-NO complex of NOS

NADPH nicotinamide adenine dinucleotide phosphate, reduced form

NOS nitric oxide synthase

NIH-PA Author Manuscript NIH-PA Author Manuscript NIH-PA Author Manuscript

NIH-PA Author Manuscript

nNOS	neuronal nitric-oxide synthase
nNOSoxy	oxygenase domain of the neuronal nitric-oxide synthase
iNOS	inducible nitric-oxide synthase
iNOSoxy	oxygenase domain of the inducible nitric-oxide synthase
WT	wild-type.

Acknowledgments

We would like to thank Allison Janocha and Serpil Erzurum for their assistance on the chemiluminescence assays. This work was supported by National Institutes of Health Grants CA53914, GM51491, and HL76491 to D.J.S. J.T. is supported by a postdoctoral fellowship (0625632B) from the American Heart Association.

References

1. Pfeiffer S, Mayer B, Hemmens B. Nitric Oxide: Chemical Puzzles Posed by a Biological Messenger. Angew. Chem. Int. Ed. 1999; 38:1714–1731.
2. Alderton WK, Cooper CE, Knowles RG. Nitric oxide synthases: structure, function and inhibition. Biochem. J. 2001; 357:593–615. [PubMed: 11463332]
3. Stuehr DJ, Santolini J, Wang ZQ, Wei CC, Adak S. Update on mechanism and catalytic regulation in the NO synthases. J. Biol. Chem. 2004; 279:36167–36170. [PubMed: 15133020]
4. Gorren ACF, Mayer B. Nitric-oxide synthase: A cytochrome P450 family foster child. Biochimica et Biophysica Acta-General Subjects. 2007; 1770:432–445.
5. Stuehr DJ, Kwon NS, Nathan CF, Griffith OW, Feldman PL, Wiseman J. N omega-hydroxy-L-arginine is an intermediate in the biosynthesis of nitric oxide from L-arginine. J. Biol. Chem. 1991; 266:6259–6263. [PubMed: 1706713]
6. Shatalin K, Gusarov I, Avetissova E, Shatalina Y, McQuade LE, Lippard SJ, Nudler E. Bacillus anthracis-derived nitric oxide is essential for pathogen virulence and survival in macrophages. Proc. Natl. Acad. Sci. U. S. A. 2008; 105:1009–1013. [PubMed: 18215992]
7. Crane BR. The enzymology of nitric oxide in bacterial pathogenesis and resistance. Biochem. Soc. Trans. 2008; 36:1149–1154. [PubMed: 19021514]
8. Negrerie M, Berka V, Vos MH, Liebl U, Lambry JC, Tsai AL, Martin JL. Geminate recombination of nitric oxide to endothelial nitric-oxide synthase and mechanistic implications. J. Biol. Chem. 1999; 274:24694–24702. [PubMed: 10455137]
9. Abu-Soud HM, Wang J, Rousseau DL, Fukuto JM, Ignarro LJ, Stuehr DJ. Neuronal nitric oxide synthase self-inactivates by forming a ferrous-nitrosyl complex during aerobic catalysis. J. Biol. Chem. 1995; 270:22997–23006. [PubMed: 7559438]
10. Santolini J, Adak S, Curran CM, Stuehr DJ. A kinetic simulation model that describes catalysis and regulation in nitric-oxide synthase. J. Biol. Chem. 2001; 276:1233–1243. [PubMed: 11038356]
11. Santolini J, Meade AL, Stuehr DJ. Differences in three kinetic parameters underpin the unique catalytic profiles of nitric-oxide synthases I, II, and III. J. Biol. Chem. 2001; 276:48887–48898. [PubMed: 11684690]
12. Adak S, Wang Q, Stuehr DJ. Molecular basis for hyperactivity in tryptophan 409 mutants of neuronal NO synthase. J. Biol. Chem. 2000; 275:17434–17439. [PubMed: 10747960]
13. Abu-Soud HM, Gachhui R, Raushel FM, Stuehr DJ. The ferrous-dioxy complex of neuronal nitric oxide synthase. Divergent effects of L-arginine and tetrahydrobiopterin on its stability. J. Biol. Chem. 1997; 272:17349–17353. [PubMed: 9211873]
14. Ghosh DK, Wu C, Pitters E, Moloney M, Werner ER, Mayer B, Stuehr DJ. Characterization of the inducible nitric oxide synthase oxygenase domain identifies a 49 amino acid segment required for subunit dimerization and tetrahydrobiopterin interaction. Biochemistry. 1997; 36:10609–10619. [PubMed: 9271491]

NIH-PA Author Manuscript NIH-PA Author Manuscript NIH-PA Author Manuscript

15. Stuehr DJ, Ikeda-Saito M. Spectral characterization of brain and macrophage nitric oxide synthases. Cytochrome P-450-like hemeproteins that contain a flavin semiquinone radical. J. Biol. Chem. 1992; 267:20547–20550. [PubMed: 1383204]
16. Scheele JS, Bruner E, Kharitonov VG, Martasek P, Roman LJ, Masters BS, Sharma VS, Magde D. Kinetics of NO ligation with nitric-oxide synthase by flash photolysis and stopped-flow spectrophotometry. J. Biol. Chem. 1999; 274:13105–13110. [PubMed: 10224063]
17. Moore EG, Gibson QH. Cooperativity in the dissociation of nitric oxide from hemoglobin. J. Biol. Chem. 1976; 251:2788–2794. [PubMed: 1262343]
18. Battino, R. IUPAC Solubility Data Series, Vol.7, Oxygen and Ozone. Oxford, England: Pergamon Press; 1981.
19. Dweik RA, Laskowski D, bu-Soud HM, Kaneko F, Hutte R, Stuehr DJ, Erzurum SC. Nitric oxide synthesis in the lung. Regulation by oxygen through a kinetic mechanism. J. Clin. Invest. 1998; 101:660–666. [PubMed: 9449700]
20. Stevenson TH, Gutierrez AF, Alderton WK, Lian L, Scrutton NS. Kinetics of CO binding to the haem domain of murine inducible nitric oxide synthase: differential effects of haem domain ligands. Biochem. J. 2001; 358:201–208. [PubMed: 11485568]
21. Sato H, Nomura S, Sagami I, Ito O, Daff S, Shimizu T. CO binding studies of nitric oxide synthase: effects of the substrate, inhibitors and tetrahydrobiopterin. FEBS Lett. 1998; 430:377–380. [PubMed: 9688574]
22. Bengea S, Araki Y, Ito O, Igarashi J, Sagami I, Shimizu T. Analysis of the kinetics of CO binding to neuronal nitric oxide synthase by flash photolysis: dual effects of substrates, inhibitors, and tetrahydrobiopterin. J. Inorg. Biochem. 2004; 98:1210–1216. [PubMed: 15219987]
23. Abu-Soud HM, Wu C, Ghosh DK, Stuehr DJ. Stopped-flow analysis of CO and NO binding to inducible nitric oxide synthase. Biochemistry. 1998; 37:3777–3786. [PubMed: 9521697]
24. Andersen HJ, Skibsted LH. Kinetics and mechanism of thermal oxidation and photooxidation of nitrosylmyoglobin in aqueous solution. J. Agric. Food Chem. 1992; 40:1741–1750.
25. Arnold EV, Bohle DS. Isolation and oxygenation reactions of nitrosylmyoglobins. Methods Enzymol. 1996; 269:41–55. [PubMed: 8791636]
26. Moller JK, Skibsted LH. Mechanism of nitrosylmyoglobin autoxidation: temperature and oxygen pressure effects on the two consecutive reactions. Chemistry. 2004; 10:2291–2300. [PubMed: 15112219]
27. Herold S, Rock G. Mechanistic studies of the oxygen-mediated oxidation of nitrosylhemoglobin. Biochemistry. 2005; 44:6223–6231. [PubMed: 15835910]
28. Marechal A, Mattioli TA, Stuehr DJ, Santolini J. Activation of peroxynitrite by inducible nitric-oxide synthase: a direct source of nitrative stress. J. Biol. Chem. 2007; 282:14101–14112. [PubMed: 17369257]
29. Ilan YA, Czapski G, Meisel D. The one-electron transfer redox potentials of free radicals. I. The oxygen/superoxide system. Biochim. Biophys. Acta. 1976; 430:209–224. [PubMed: 179587]
30. Ost TW, Daff S. Thermodynamic and kinetic analysis of the nitrosyl, carbonyl, and dioxy heme complexes of neuronal nitric-oxide synthase. The roles of substrate and tetrahydrobiopterin in oxygen activation. J. Biol. Chem. 2005; 280:965–973. [PubMed: 15507439]
31. Ray SS, Tejero J, Wang ZQ, Dutta T, Bhattacharjee A, Regulski M, Tully T, Ghosh S, Stuehr DJ. Oxygenase domain of Drosophila melanogaster nitric oxide synthase: unique kinetic parameters enable a more efficient NO release. Biochemistry. 2007; 46:11857–11864. [PubMed: 17900148]
32. Cooper CE. Nitric oxide and iron proteins. Biochim. Biophys. Acta. 1999; 1411:290–309. [PubMed: 10320664]
33. Andersen JF, Ding XD, Balfour C, Shokhireva TK, Champagne DE, Walker FA, Montfort WR. Kinetics and equilibria in ligand binding by nitrophorins 1–4: evidence for stabilization of a nitric oxide-ferriheme complex through a ligand-induced conformational trap. Biochemistry. 2000; 39:10118–10131. [PubMed: 10956000]
34. De Marinis E, Casella L, Ciaccio C, Coletta M, Visca P, Ascenzi P. Catalytic peroxidation of nitrogen monoxide and peroxynitrite by globins. IUBMB. Life. 2009; 61:62–73. [PubMed: 19109828]

NIH-PA Author Manuscript
NIH-PA Author Manuscript
NIH-PA Author Manuscript

35. Fasano M, Antonini G, Ascenzi P. O2-mediated oxidation of hemopexin-heme(II)-NO. Biochem. Biophys. Res. Commun. 2006; 345:704–712. [PubMed: 16696943]
36. Herold S, Fago A, Weber RE, Dewilde S, Moens L. Reactivity studies of the Fe(III) and Fe(II)NO forms of human neuroglobin reveal a potential role against oxidative stress. J. Biol. Chem. 2004; 279:22841–22847. [PubMed: 15020597]
37. Gardner PR. Nitric oxide dioxygenase function and mechanism of flavohemoglobin, hemoglobin, myoglobin and their associated reductases. J. Inorg. Biochem. 2005; 99:247–266. [PubMed: 15598505]
38. Frey AD, Kallio PT. Bacterial hemoglobins and flavohemoglobins: versatile proteins and their impact on microbiology and biotechnology. FEMS Microbiol. Rev. 2003; 27:525–545. [PubMed: 14550944]
39. Gardner AM, Martin LA, Gardner PR, Dou Y, Olson JS. Steady-state and transient kinetics of Escherichia coli nitric-oxide dioxygenase (flavohemoglobin). The B10 tyrosine hydroxyl is essential for dioxygen binding and catalysis. J. Biol. Chem. 2000; 275:12581–12589. [PubMed: 10777548]
40. Gardner PR, Gardner AM, Martin LA, Dou Y, Li T, Olson JS, Zhu H, Riggs AF. Nitric-oxide dioxygenase activity and function of flavohemoglobins. sensitivity to nitric oxide and carbon monoxide inhibition. J. Biol. Chem. 2000; 275:31581–31587. [PubMed: 10922365]
41. Hausladen A, Gow A, Stamler JS. Flavohemoglobin denitrosylase catalyzes the reaction of a nitroxyl equivalent with molecular oxygen. Proc. Natl. Acad. Sci. U. S. A. 2001; 98:10108–10112. [PubMed: 11517313]
42. Gardner PR, Gardner AM, Martin LA, Salzman AL. Nitric oxide dioxygenase: an enzymic function for flavohemoglobin. Proc. Natl. Acad. Sci. U. S. A. 1998; 95:10378–10383. [PubMed: 9724711]
43. Hausladen A, Gow AJ, Stamler JS. Nitrosative stress: metabolic pathway involving the flavohemoglobin. Proc. Natl. Acad. Sci. U. S. A. 1998; 95:14100–14105. [PubMed: 9826660]
44. Rinaldo S, Arcovito A, Brunori M, Cutruzzola F. Fast dissociation of nitric oxide from ferrous Pseudomonas aeruginosa cd1 nitrite reductase. A novel outlook on the catalytic mechanism. J. Biol. Chem. 2007; 282:14761–14767. [PubMed: 17389587]
45. Sam KA, Fairhurst SA, Thorneley RN, Allen JW, Ferguson SJ. Pseudoazurin dramatically enhances the reaction profile of nitrite reduction by Paracoccus pantotrophus cytochrome cd1 and facilitates release of product nitric oxide. J. Biol. Chem. 2008; 283:12555–12563. [PubMed: 18310770]
46. Quaroni LG, Seward HE, McLean KJ, Girvan HM, Ost TW, Noble MA, Kelly SM, Price NC, Cheesman MR, Smith WE, Munro AW. Interaction of nitric oxide with cytochrome P450 BM3. Biochemistry. 2004; 43:16416–16431. [PubMed: 15610036]
47. Morgan ET, Ullrich V, Daiber A, Schmidt P, Takaya N, Shoun H, McGiff JC, Oyekan A, Hanke CJ, Campbell WB, Park CS, Kang JS, Yi HG, Cha YN, Mansuy D, Boucher JL. Cytochromes P450 and flavin monooxygenases--targets and sources of nitric oxide. Drug Metab Dispos. 2001; 29:1366–1376. [PubMed: 11602511]
48. Aguiar M, Masse R, Gibbs BF. Regulation of cytochrome P450 by posttranslational modification. Drug Metab Rev. 2005; 37:379–404. [PubMed: 15931769]
49. Aulak KS, Miyagi M, Yan L, West KA, Massillon D, Crabb JW, Stuehr DJ. Proteomic method identifies proteins nitrated in vivo during inflammatory challenge. Proc. Natl. Acad. Sci. U. S. A. 2001; 98:12056–12061. [PubMed: 11593016]
50. Xia Y, Zweier JL. Superoxide and peroxynitrite generation from inducible nitric oxide synthase in macrophages. Proc. Natl. Acad. Sci. U. S. A. 1997; 94:6954–6958. [PubMed: 9192673]
51. Adak S, Bilwes AM, Panda K, Hosfield D, Aulak KS, McDonald JF, Tainer JA, Getzoff ED, Crane BR, Stuehr DJ. Cloning, expression, and characterization of a nitric oxide synthase protein from Deinococcus radiodurans. Proc. Natl. Acad. Sci. U. S. A. 2002; 99:107–112. [PubMed: 11756668]
52. Kers JA, Wach MJ, Krasnoff SB, Widom J, Cameron KD, Bukhalid RA, Gibson DM, Crane BR, Loria R. Nitration of a peptide phytotoxin by bacterial nitric oxide synthase. Nature. 2004; 429:79–82. [PubMed: 15129284]

53. Abu-Soud HM, Rousseau DL, Stuehr DJ. Nitric oxide binding to the heme of neuronal nitric-oxide synthase links its activity to changes in oxygen tension. J. Biol. Chem. 1996; 271:32515–32518. [PubMed: 8955074]

54. Guo FH, De Raeve HR, Rice TW, Stuehr DJ, Thunnissen FB, Erzurum SC. Continuous nitric oxide synthesis by inducible nitric oxide synthase in normal human airway epithelium in vivo. Proc. Natl. Acad. Sci. U. S. A. 1995; 92:7809–7813. [PubMed: 7544004]

55. Salerno JC. Neuronal nitric oxide synthase: prototype for pulsed enzymology. FEBS Lett. 2008; 582:1395–1399. [PubMed: 18396171]

56. Van Doorslaer S, Dewilde S, Kiger L, Nistor SV, Goovaerts E, Marden MC, Moens L. Nitric oxide binding properties of neuroglobin - A characterization by EPR and flash photolysis. Journal of Biological Chemistry. 2003; 278:4919–4925. [PubMed: 12480932]

57. Kharitonov VG, Sharma VS, Magde D, Koesling D. Kinetics of nitric oxide dissociation from five- and six-coordinate nitrosyl hemes and heme proteins, including soluble guanylate cyclase. Biochemistry. 1997; 36:6814–6818. [PubMed: 9184164]

58. Sarti P, Giuffre A, Forte E, Mastronicola D, Barone MC, Brunori M. Nitric oxide and cytochrome c oxidase: mechanisms of inhibition and NO degradation. Biochem. Biophys. Res. Commun. 2000; 274:183–187. [PubMed: 10903916]

NIH-PA Author Manuscript

NIH-PA Author Manuscript

NIH-PA Author Manuscript

NIH-PA Author Manuscript
NIH-PA Author Manuscript
NIH-PA Author Manuscript

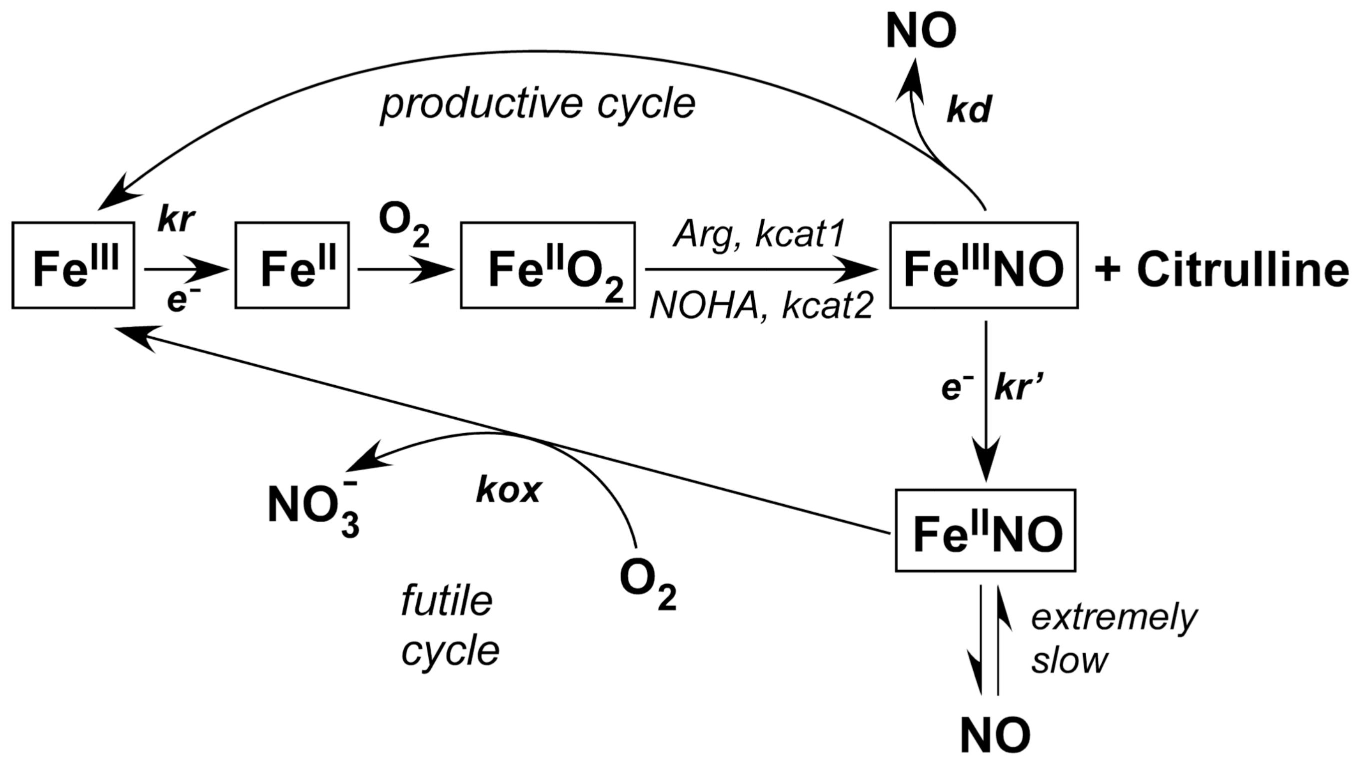

Figure 1.

NIH-PA Author Manuscript
NIH-PA Author Manuscript
NIH-PA Author Manuscript

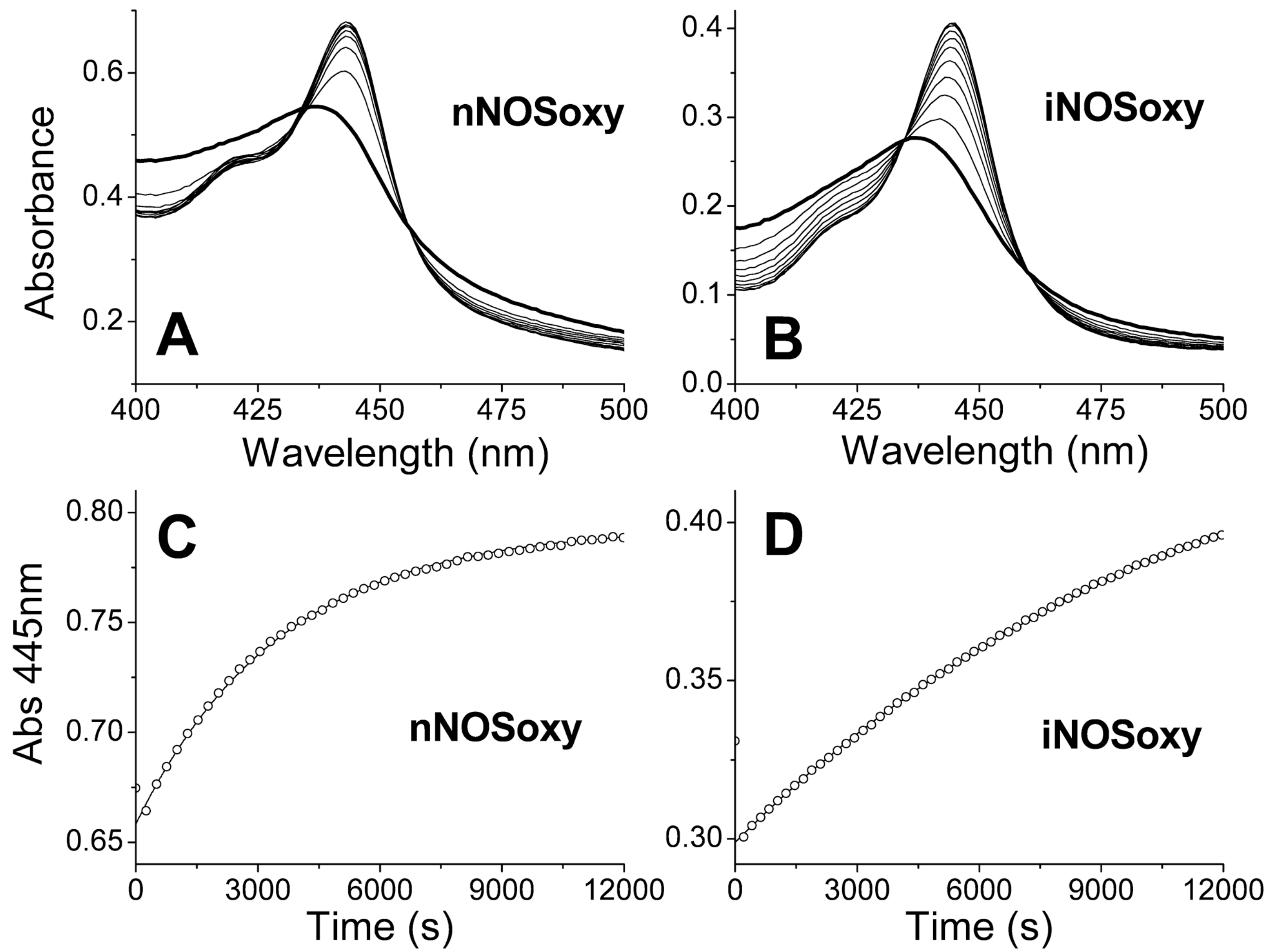

Figure 2.

NIH-PA Author Manuscript

NIH-PA Author Manuscript

NIH-PA Author Manuscript

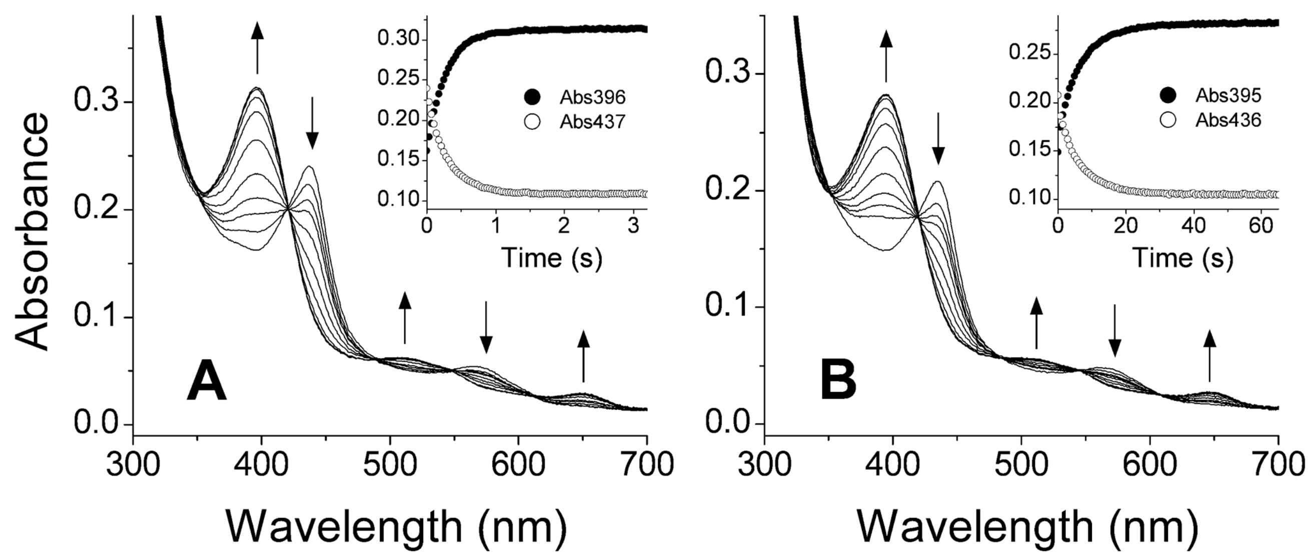

Figure 3.

NIH-PA Author Manuscript
NIH-PA Author Manuscript
NIH-PA Author Manuscript

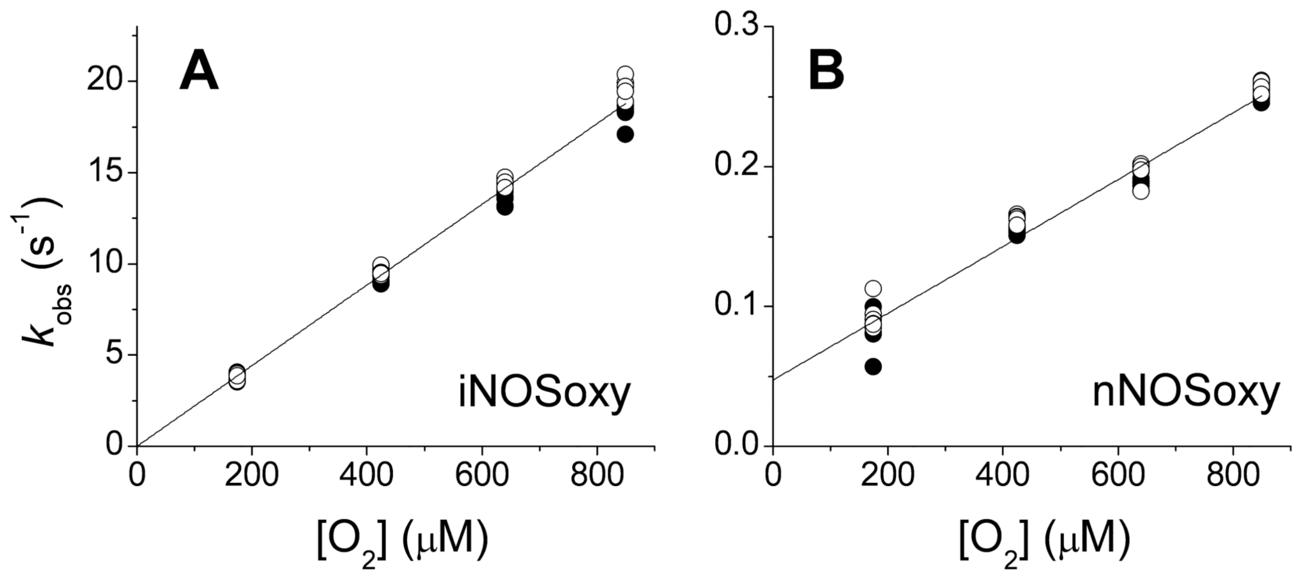

Figure 4.

NIH-PA Author Manuscript
NIH-PA Author Manuscript
NIH-PA Author Manuscript

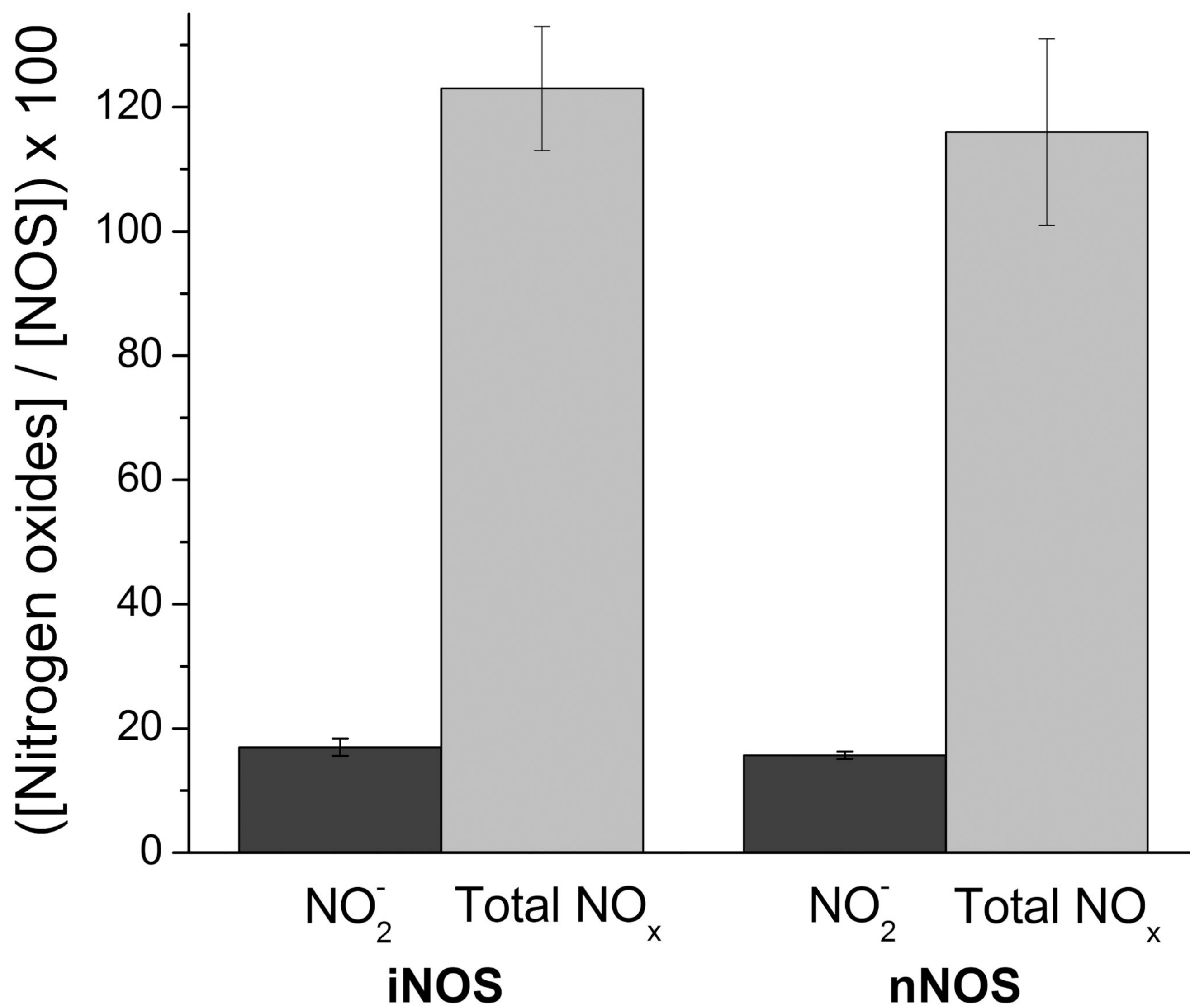

Figure 5.

NIH-PA Author Manuscript
NIH-PA Author Manuscript
NIH-PA Author Manuscript

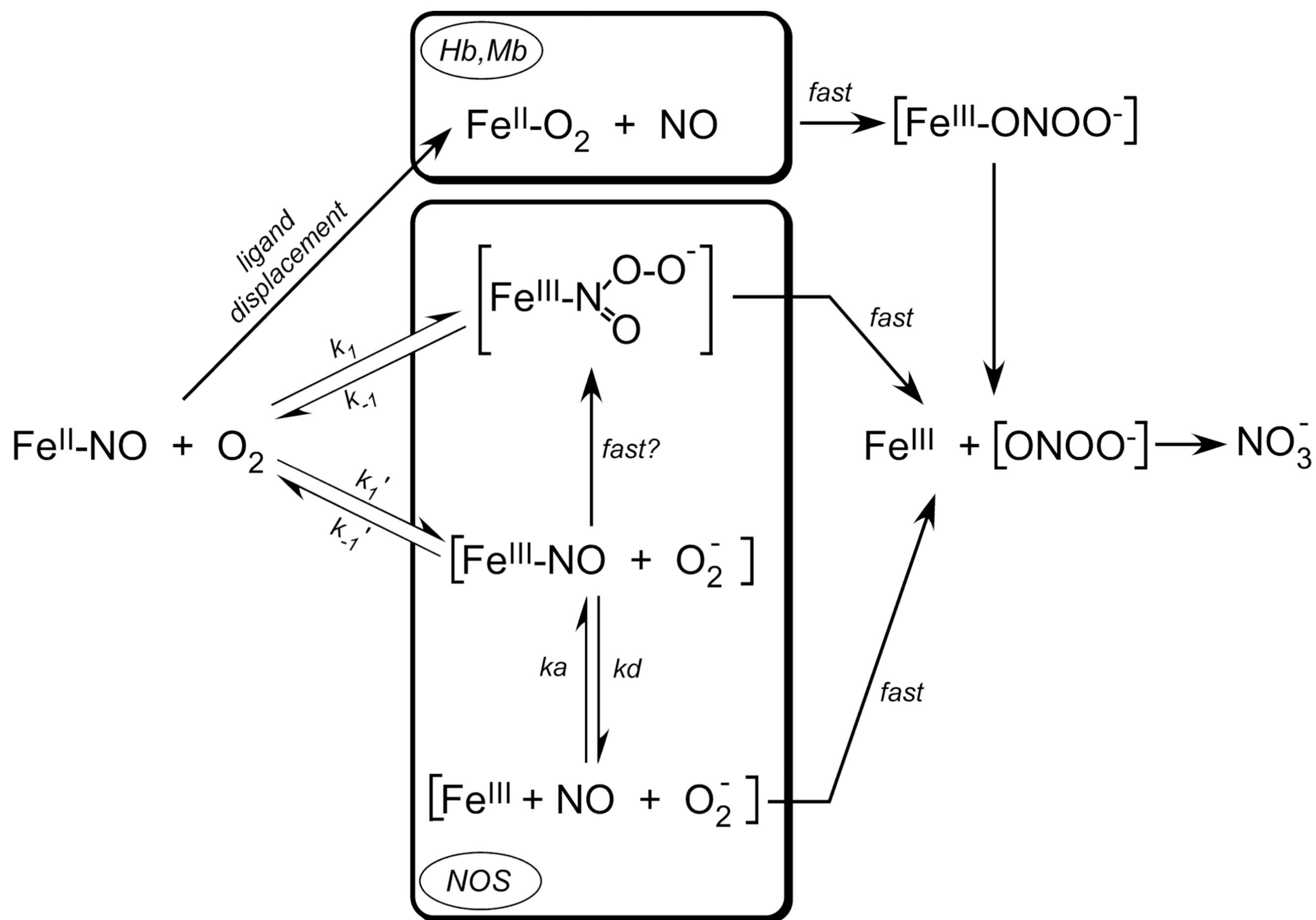

Figure 6.

NIH-PA Author Manuscript
NIH-PA Author Manuscript
NIH-PA Author Manuscript

Table 1

Rates of Ferrous Heme-NO dissociation and oxidation for NOSoxy and other heme proteins.

Protein	NO dissociation	NO oxidation [a]		References
iNOSoxy	1.0×10^{-4} s^{-1}	$k_1 = 2.65 \times 10^4$ M^{-1}s^{-1}		Present study
nNOSoxy	3.9×10^{-4} s^{-1}	$k_1 = 2.30 \times 10^2$ M^{-1}1s^{-1}	$k_{-1} = 4.7 \times 10^{-2}$ s^{-1}	Present study
Neuroglobin	2.0×10^{-4} s^{-1}	$k_1 = 1.6 \times 10^1$ M^{-1}s^{-1}	$k_2 = 5.0 \times 10^{-4}$ s^{-1}	[36;56]
Hemopexin	9.1×10^{-4} s^{-1}	$k_1 = 2.4\times 10^1$ M^{-1}s^{-1}	$k_2 = 1.4 \times 10^{-3}$ s^{-1}	[35]
Myoglobin	0.9×10^{-5} s^{-1}	$k_1 = 1.3 \times 10^{-4}$ s^{-1}	$k_2 = 2.6 \times 10^{-4}$ s^{-1}	[26;57]
Hemoglobin	3.2×10^{-4} s^{-1} [b]	$k_1 = 2.0 \times 10^{-4}$ s^{-1}	$k_2 = 1.0 \times 10^{-4}$ s^{-1}	[27]
Guanylate cyclase	7.0×10^{-4} s^{-1}			[57]
Cytochrome *c* oxidase	1.0×10^{-2} s^{-1}			[58]
Cytochrome *cd*1	4.35×10^1 s^{-1}			[44]

[a] The second kinetic parameters are referred to as k_{-1} and k_2 because in the case of nNOS it reflects an apparent equilibrium and in the other proteins refers to a subsequent reaction.

[b] This is the fast rate; bi-exponential fit gave values of: k_1=3.2 × 10^{-4} s^{-1}; k_2 = 0.7 × 10^{-4} s^{-1} [27].